

(NASA-TM-83879) MOTION OF THE ANGULAR  
MOMENTUM VECTOR IN BODY COORDINATES FOR  
TORQUE-FREE DUAL-SPIN SPACECRAFT (NASA)  
26 p HC A03/MF A01

CSCI 22B

N82-24282

Unclas  
G3/18 21222



## Technical Memorandum 83879

# Motion of the Angular Momentum Vector in Body Coordinates for Torque-Free Dual-Spin Spacecraft

Joseph V. Fedor

DECEMBER 1981

National Aeronautics and  
Space Administration

Goddard Space Flight Center  
Greenbelt, Maryland 20771



**TM 83879**

**MOTION OF THE ANGULAR MOMENTUM VECTOR IN BODY  
COORDINATES FOR TORQUE-FREE DUAL-SPIN SPACECRAFT**

**Joseph V. Fedor**

**December 1981**

**GODDARD SPACE FLIGHT CENTER  
Greenbelt, Maryland**

## MOTION OF THE ANGULAR MOMENTUM VECTOR IN BODY COORDINATES FOR TORQUE-FREE DUAL-SPIN SPACECRAFT

Joseph V. Fedor

### ABSTRACT

A solution is developed for the motion of the angular momentum vector in body coordinates for torque-free, asymmetric dual-spin spacecraft without and, for a special case, with energy dissipation on the main spacecraft. Without energy dissipation, two integrals can be obtained from the Euler equations of motion. Using the classical method of elimination of variable, the motion about the equilibrium points (six for the general case) are derived with these integrals. For small nutation angle,  $\theta$ , the trajectories about the  $\theta = 0^\circ$  and  $\theta = 180^\circ$  points readily show the requirements for stable motion about these points. Also the conditions needed to eliminate stable motion about the  $\theta = 180^\circ$  point as well as the other undesirable equilibrium points follow directly from these equations. These requirements are in agreement with C. Hubert (Reference 1).

For the special case where the angular momentum vector moves about the principal axis which contains the momentum wheel, the notion of "free variable" azimuth angle is used. Physically this angle must vary from 0 to  $2\pi$  in a circular periodic fashion. Expressions are thus obtained for the nutation angle in terms of the free variable and other spacecraft parameters. Results for this case show that in general there are two separate trajectory expressions that govern the motion of the angular momentum vector in body coordinates. If the relative angular momentum ratio,  $h/H$ , satisfies certain inequalities (conditions), one trajectory can be eliminated from consideration. Other expressions developed in the paper such as extreme values of the nutation angle in a cycle of motion and permissible limits on a dimensionless momentum-energy parameter,  $H^2/2TC$ , reduces to the classical results for spinning torque-free rigid body when the rotor angular momentum is set to zero. Energy dissipation on the spacecraft is simulated by a liquid filled ring damper, and a simple computer program has been generated that allows the user to determine the motion of the angular momentum vector in body coordinates for the special case. Typical trajectories are exhibited. Also, for small nutation angles, a relationship is expressed between the free variable and time, and a damping time constant is derived.

## CONTENTS

	<u>Page</u>
ABSTRACT .....	iii
1. INTRODUCTION .....	1
2. ANALYSIS WITHOUT ENERGY DISSIPATION .....	1
3. ANGULAR MOMENTUM VECTOR MOTION ABOUT THE 3 AXIS .....	9
4. ENERGY DISSIPATION ON THE MAIN SPACECRAFT .....	12
5. NUMERICAL RESULTS .....	15
6. SUMMARY .....	16
7. REFERENCES .....	20
APPENDIX A: CSMP PROGRAM FOR MOTION OF THE ANGULAR MOMENTUM VECTOR ABOUT THE AXIS THAT CONTAINS THE MOMENTUM WHEEL .....	21

## ILLUSTRATIONS

<u>Figure</u>	<u>Page</u>
1 General orientation of a unit angular momentum vector in body fixed normalized momentum coordinates .....	2
2 Loci of the angular momentum vector for a dual-spin spacecraft on a portion of a momentum ellipsoid for $A < B < C$ inertia distribution and $h/H > 0$ .....	9
3 Polar plot of nutation angle versus free variable, $\alpha$ , for small motion about the $\theta = 0^\circ$ point, $R_1 = 0.03$ , $R_3 = 0.0, 0.1$ .....	17
4 Nutation angle versus free variable, $\alpha$ , for $R_1 = 0.03$ and $R_3 = 0.1$ for $\theta_0 =$ $45^\circ, 90^\circ, 135^\circ, 170^\circ$ .....	18
5 Nutation angle versus free variable, $\alpha$ , for $R_1 = 0.09$ and $R_3 = 0.1$ for $\theta_0 =$ $135^\circ, 170^\circ$ .....	19

# MOTION OF THE ANGULAR MOMENTUM VECTOR IN BODY COORDINATES FOR TORQUE-FREE DUAL-SPIN SPACECRAFT

## 1. INTRODUCTION

The attitude motion of dual-spin spacecraft has been examined in considerable detail (References 1-5, to mention a few) with various mathematical techniques. There appears to be a lack, though, of a simple, direct analysis of torque-free, asymmetric dual-spin spacecraft attitude motion, unencumbered with complicated mathematical details, that reveals the nature of the motion and blends in with the well known classical results of spinning torque-free situation. It is the intent of this paper to present such an analysis. First, the torque-free situation without energy dissipation will be examined and then, for a special case, energy dissipation in the form of a liquid ring damper on the main spacecraft will be included.

## 2. ANALYSIS WITHOUT ENERGY DISSIPATION

Using a 1-2-3 principal axis coordinate system fixed in the spacecraft and with the origin at the center of mass of the spacecraft, the angular momentum of the system,  $\vec{H}$ , can be written as

$$\vec{H} = \begin{pmatrix} A\omega_1 \\ B\omega_2 \\ C\omega_3 + h \end{pmatrix}$$

where A, B and C are the principal moments of inertia,  $\omega_1, \omega_2, \omega_3$  are the components of the angular velocity vector and h is the relative angular momentum of the wheel which is located on the 3 axis. A perfect control system is assumed which keeps the wheel speed constant and hence h. The vector equation of motion can be written as

$$\dot{\vec{H}} + \vec{\omega} \times \vec{H} = 0 \quad (1)$$

In scalar form, Equation 1 can be written as

$$A\dot{\omega}_1 + (C - B)\omega_2\omega_3 + h\omega_2 = 0 \quad (2)$$

$$B\dot{\omega}_2 + (A - C)\omega_1\omega_3 - h\omega_1 = 0 \quad (3)$$

$$C\dot{\omega}_3 + (B - A)\omega_1\omega_2 = 0 \quad (4)$$

Multiplying Equation 2 by  $\omega_1$ , Equation 3 by  $\omega_2$  and Equation 4 by  $\omega_3$ , adding and noting that the resulting expression is an exact differential which can be integrated gives

$$A\omega_1^2 + B\omega_2^2 + C\omega_3^2 = 2T = \text{Constant} \quad (5)$$

Equation 5 is the rotational energy of the spacecraft with the momentum wheel not rotating and it is a constant of the motion. Another constant of the motion, since the motion is torque-free, is the magnitude of the angular momentum vector

$$(A\omega_1)^2 + (B\omega_2)^2 + (C\omega_3 + h)^2 = H^2 = \text{Constant} \quad (6)$$

Note also, that because of the torque-free nature of the motion, the angular momentum vector is fixed in space and can be used as a reference direction to ascertain external viewed motion.

Referring to Figure 1 which shows a general orientation of a unit angular momentum vector in body fixed normalized momentum coordinates

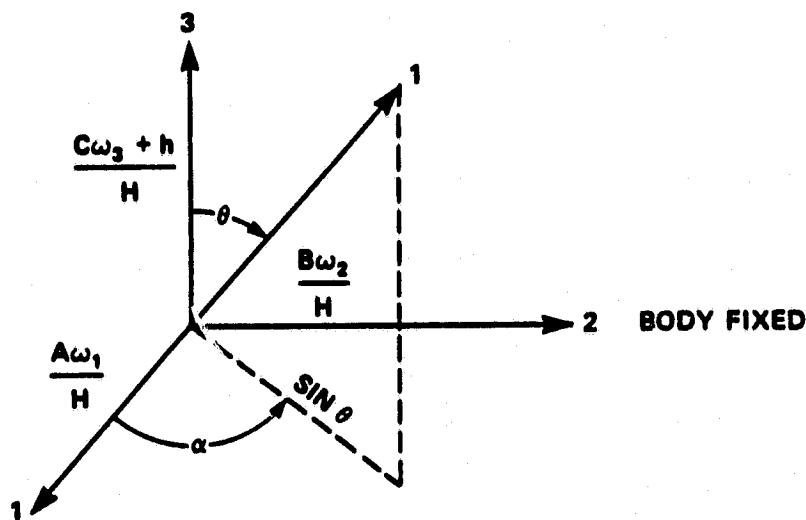


Figure 1. General orientation of a unit angular momentum vector in body fixed normalized momentum coordinates.

one can write

$$\frac{A\omega_1}{H} = \sin \theta \cos \alpha \text{ or } \omega_1 = \frac{H}{A} \sin \theta \cos \alpha \quad (7)$$

$$\frac{B\omega_2}{H} = \sin \theta \sin \alpha \text{ or } \omega_2 = \frac{H}{B} \sin \theta \sin \alpha \quad (8)$$

$$\frac{C\omega_3 + h}{H} = \cos \theta \text{ or } \omega_3 = \frac{H \cos \theta - h}{C} \quad (9)$$

The angle  $\theta$  is the conventional nutation angle and  $\alpha$  is an azimuth angle. When the normalized components of the angular momentum are substituted in Equation 6, the conservation of angular momentum equation, it will be found that this equation is satisfied exactly. This fact is used in subsequent development.

The equilibrium points of the motion will now be obtained using the two integrals of motion and the method of elimination of variable. First  $A\omega_1$  will be eliminated which corresponds to viewing the motion along the 1 axis, then  $B\omega_2$  which corresponds to viewing the motion along the 2 axis and finally  $C\omega_3 + h$ . Equation 9 is used to write the conservation of angular momentum as follows

$$H^2 = (A\omega_1)^2 + (B\omega_2)^2 + H^2 \cos^2 \theta \quad (10)$$

and the rotational energy equation as

$$2T = A\omega_1^2 + B\omega_2^2 + \frac{H^2}{C} (\cos \theta - R_1)^2 \quad (11)$$

Where  $R_1 = h/H$ , the relative angular momentum ratio of the rotor.  $\omega_1$  can be eliminated by multiplying Equation 11 by  $A$  and subtracting it from Equation 10; this gives the following

$$H^2 - 2AT = (1 - A/B)(B\omega_2)^2 + H^2 \left\{ \cos^2 \theta - \frac{A}{C} (\cos \theta - R_1)^2 \right\} \quad (12)$$

Now the expression in the braces can be written as a perfect square containing  $\cos \theta$  and some residual constant terms. Thus after some rearranging, Equation 12 becomes

$$(1 - A/B) \left( \frac{B\omega_2}{H} \right)^2 + (1 - A/C) \left( \cos \theta - \frac{R_1}{1 - C/A} \right)^2 = \frac{1}{R_2} \left[ R_2 \left( 1 + \frac{R_1^2}{C/A - 1} \right) - \frac{A}{C} \right] \quad (13)$$

where  $R_2$  is defined as

$$R_2 = \frac{H^2}{2TC} \quad (14)$$

As noted previously, Equation 13 represents motion projected on a plane normal to the 1 axis of the body fixed coordinate system. It will be noted that the equilibrium point is at

$$\cos \theta = \frac{R_1}{1 - C/A}, \quad (15)$$

$\omega_2 = 0$  (which implies  $\alpha = 0$  or  $\pi$ ) and

$$R_2 = \frac{A}{C} \frac{(C/A - 1)}{(C/A - 1 + R_1^2)} \quad (16)$$

Now Equation 13 is a displaced conic section locus, and it can be either an ellipse or a hyperbola. For an inertia distribution of:  $A < B < C$ , the coefficients of the left side squared terms are positive and so closed path ellipse trajectories are possible about the equilibrium point for positive right hand side, which requires that

$$R_2 > \frac{A}{C} \frac{(C/A - 1)}{(C/A - 1 + R_1^2)} \quad (17)$$

In a similar manner for the 2 axis, one can derive the following expression

$$(1 - B/A) \left( \frac{A\omega_1}{H} \right)^2 + (1 - B/C) \left( \cos \theta - \frac{R_1}{1 - C/B} \right)^2 = \frac{1}{R_2} \left[ R_2 \left( 1 + \frac{R_1^2}{C/B - 1} \right) - \frac{B}{C} \right] \quad (18)$$

Again it will be observed, that for this axis the equilibrium point is at

$$\cos \theta = \frac{R_1}{1 - C/B}, \quad (19)$$

$\omega_1 = 0$  (which implies  $\alpha = \pm\pi/2$ ) and

$$R_2 = \frac{B}{C} \frac{(C/B - 1)}{(C/B - 1 + R_1^2)} \quad (20)$$



For the stated inertia distribution, it can be seen from Equation 18 that one coefficient of the squared terms on the left side is negative and so the motion about this point is hyperbola in nature. The slopes of the asymptotes in a plane normal to the 2 axis are given by

$$\frac{\left(\cos \theta - \frac{R_1}{1 - C/B}\right)}{\left(\frac{A\omega_1}{H}\right)} = \pm \sqrt{\frac{C}{A} \frac{(B - A)}{(C - B)}} \quad (21)$$

These represent separatrices as projected on the 1-3 plane. If the equilibrium point exists, then the above implies that no closed path motion will take place about this point. Note further, that these separatrices (right hand side) are identical to the simple spinning torque-free case (Reference 6).

For the two equilibrium points just described, it is interesting to note that compared to the simple spinning torque-free case, the presence of a momentum wheel changes the location of these equilibrium points only in the  $\theta$  direction and not in the azimuth ( $\alpha$ ) direction. Further, as the relative angular momentum of the wheel increases from zero (note Equation 15 and 19) the equilibrium points migrate toward the  $\theta = 0^\circ$  or  $180^\circ$  points, and if the rotor momentum is high enough as required by the following

$$R_1 > |1 - C/A| \quad (22a)$$

and

$$R_1 > |1 - C/B| \quad (22b)$$

the equilibrium points are eliminated (not realizable). This has implications for all attitude angle acquisition which will be discussed somewhat more further on in the paper.

For motion as viewed along the 3 axis, Equation 11 is multiplied by C and Equation 10 is subtracted from it which eliminates  $H^2 \cos^2 \theta$  and gives the following intermediate result

$$(C/A - 1)(A\omega_1)^2 + (C/B - 1)(B\omega_2)^2 - H^2(2R_1 \cos \theta - R_1^2) = 2TC - H^2 \quad (23)$$

Now Equation 10 can also be written as

$$\cos \theta = \pm \left( 1 - \frac{[(A\omega_1)^2 + (B\omega_2)^2]}{H^2} \right)^{1/2} \quad (24)$$

For  $\theta$  near zero,  $\cos \theta$  can be approximated by

$$\cos \theta \approx 1 - \frac{1}{2} \frac{[(A\omega_1)^2 + (B\omega_2)^2]}{H^2} \quad (25a)$$

and for  $\theta$  near  $180^\circ$ ,  $\cos \theta$  can be approximated by

$$\cos \theta \approx -1 + \frac{1}{2} \frac{[(A\omega_1)^2 + (B\omega_2)^2]}{H^2} \quad (25b)$$

Combining Equations 25a, b with Equation 23 and rearranging terms, one arrives at

$$[C/A - 1 + R_1] \left( \frac{A\omega_1}{H} \right)^2 + [C/B - 1 + R_1] \left( \frac{B\omega_2}{H} \right)^2 = [1/R_2 - (1 - R_1)^2] \quad (26)$$

for  $\theta$  near zero and

$$[C/A - 1 - R_1] \left( \frac{A\omega_1}{H} \right)^2 + [C/B - 1 - R_1] \left( \frac{B\omega_2}{H} \right)^2 = \left[ \frac{1}{R_2} - (1 + R_1)^2 \right] \quad (27)$$

for  $\theta$  near  $180^\circ$ . Equation 26 and 27 represent trajectory motion of the unit angular momentum vector if one were to look along the positive or negative 3 axis. The equilibrium points are  $\omega_1 = \omega_2 = 0$  (which implies  $\theta = 0$  or  $\pi$  for any value of  $\alpha$ ) and

$$R_2 = \frac{1}{(1 - R_1)^2} \quad (28)$$

for  $\theta = 0^\circ$ , and

$$R_2 = \frac{1}{(1 + R_1)^2} \quad (29)$$

for  $\theta = 180^\circ$ . Examining Equations 26 and 27 further, one can conclude that for  $\theta$  near zero, closed ellipse like motion is possible if

$$C/A - 1 + R_1 > 0 \quad (30a)$$

$$C/B - 1 + R_1 > 0 \quad (30b)$$

and

$$R_2 < \frac{1}{(1 - R_1)^2} \quad (30c)$$

For  $\theta$  near  $180^\circ$ , a similar type of motion is possible if

$$C/A - 1 - R_1 > 0 \quad (31a)$$

$$C/B - 1 - R_1 > 0 \quad (31b)$$

and

$$R_2 < \frac{1}{(1 + R_1)^2} \quad (31c)$$

Note that since  $T = \frac{H^2}{2R_2 C}$ , for a given spacecraft moment of inertia and angular momentum, the  $\theta = 0^\circ$  equilibrium point is a lower rotational energy point than the  $\theta = 180^\circ$  point. Also, it will be noted in Equation 27 that if the rotor relative angular momentum is made large enough (since physically  $C/A$  or  $C/B$  is less than 2) so as to make one coefficient negative, no closed path motion is possible about the  $\theta = 180^\circ$  point.

To emphasize this condition, the following is written

$$R_1 > C/A - 1 \quad (32a)$$

or

$$R_1 > C/B - 1 \quad (32b)$$

which eliminates closed path motion about the  $\theta = 180^\circ$  point. That is, if inequality 32a or 32b is satisfied, then the motion about the  $180^\circ$  point is hyperbolic in nature. If both inequalities are satisfied, then closed path motion is still possible provided that

$$R_2 > \frac{1}{(1 + R_1)^2}$$

If both inequalities are satisfied in an absolute value sense, the previously mentioned equilibrium points about the 1 and 2 axes are eliminated and the only equilibrium points are at  $\theta = 0^\circ$  and

180°. In this case  $R_2$  is bounded by the following

$$\frac{1}{(1 + R_1)^2} \leq R_2 \leq \frac{1}{(1 - R_1)^2} \quad (33)$$

Thus, without energy dissipation, depending upon the magnitude of the rotor relative angular momentum,  $R_1$ , there can be two, four or six equilibrium points for a given dual-spin spacecraft moment of inertia configuration.

It is appropriate at this point to briefly consider energy dissipation. This implies that the spacecraft rotational energy ( $T$ ) is decreasing so that  $R_2$  approaches  $\frac{1}{(1 - R_1)^2}$  (Equation 33). If  $R_2$  were to approach  $\frac{1}{(1 + R_1)^2}$ , this implies that  $T$  is increasing which is contrary to what Reference 8 has demonstrated. It is thus seen that the final steady state equilibrium is  $\theta = 0^\circ$ .

Summarizing briefly, when the appropriate inequalities are satisfied leaving the  $\theta = 0^\circ$  and the 180° point as possible equilibrium points, because the 180° point is at a higher rotational energy level, this point is also eliminated in a sense that the momentum vector will not move to that point with inexorable energy dissipation present. This leaves the  $\theta = 0^\circ$  as the only remaining equilibrium point. The above is important for all attitude acquisition as noted by Reference 1.

Another technical point can be noted from Equations 26 and 27. If the spacecraft were captured about the  $\theta = 0^\circ$  point and it is desired to invert the attitude of the spacecraft, this can be done by changing the rotor speed ( $R_1$ ) to a negative value so as to make the  $\theta = 0^\circ$  point a higher energy point and correspondingly make the  $\theta = 180^\circ$  a lower energy point. The above mentioned discussion of energy dissipation would then apply again.

To add a geometric dimension to the analytic result, Figure 2 shows a sketch of the loci of the angular momentum vector on a portion of a momentum ellipsoid for  $A < B < C$  with three equilibrium points showing (total of six present).

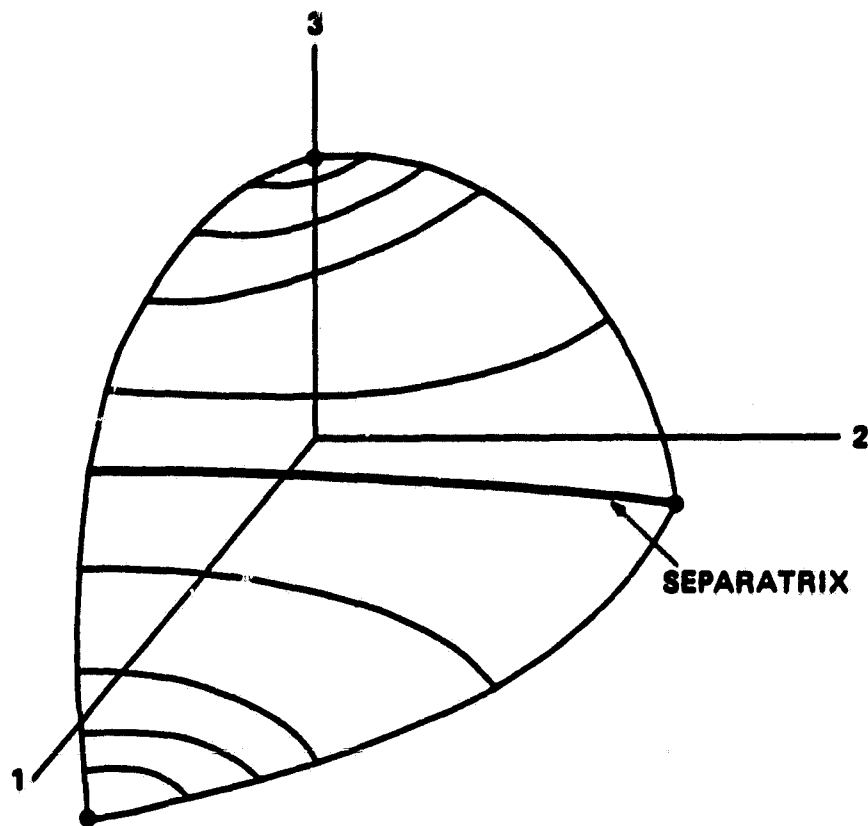


Figure 2. Loci of the angular momentum vector for a dual-spin spacecraft on a portion of a momentum ellipsoid for  $A < B < C$  inertia distribution and  $h/H > 0$ .

### 3. ANGULAR MOMENTUM VECTOR MOTION ABOUT THE 3 AXIS

Attention will now be focused on the special but significant case where the angular momentum vector moves about the principal axis that contains the momentum wheel. This will further elucidate and quantify the attitude dynamics of dual-spin spacecraft. With this motion, the azimuth angle that locates the transverse component of the angular momentum vector must vary from 0 to  $2\pi$  in a periodic manner. This angle,  $\alpha$ , is called a "free variable" and is treated as an independent variable in what follows.

As mentioned previously, when the normalized components of angular momentum (Equations 7, 8 and 9) are substituted into Equation 6, the conservation of angular momentum equation, it will be found that the equation is satisfied exactly. Substituting  $\omega_1$ ,  $\omega_2$ ,  $\omega_3$  into

Equation 5, the energy equation, and after some manipulation and definition of terms, results in a quadratic expression for the nutation angle in terms of  $\alpha$

$$G_1 \cos^2 \theta - 2R_1 \cos \theta - G_2 = 0 \quad (34)$$

where

$$G_1 = 1 - \frac{C}{A} \cos^2 \alpha - \frac{C}{B} \sin^2 \alpha \quad (35)$$

$$G_2 = \frac{1}{R_2} - R_1^2 - \frac{C}{A} \cos^2 \alpha - \frac{C}{B} \sin^2 \alpha$$

or

$$G_2 = \frac{1}{R_2} - R_1^2 + G_1 - 1 \quad (36)$$

and, as before

$$R_1 = h/H, \quad R_2 = \frac{H^2}{2TC}$$

Solving for  $\cos \theta$  in Equation 34 gives

$$\cos \theta = \frac{R_1 \pm \sqrt{R_1^2 + G_1 G_2}}{G_1} \quad (37)$$

It will be noted that because of the  $\pm$  sign, there are potentially two trajectories expressions for the nutation angle,  $\theta$ . The plus sign trajectory is an optional (possible) trajectory depending upon  $R_1$ , the relative angular momentum ratio of the rotor. This is inferred from the inequalities in Equations 32a, b. If Equation 32a or b is true, this implies  $\left| \frac{R_1}{G_1} \right| > 1$  at some azimuth points in the  $\cos \theta$  equation. The  $\frac{\sqrt{R_1^2 + G_1 G_2}}{G_1}$  component will always increase  $R_1/G_1$  in the positive sign trajectory and thus make the right hand side of Equation 37 even larger than  $\pm 1$ , which, of course, is not physically realizable and thus eliminates that trajectory from consideration. For the negative sign trajectory it is of value to let  $R_2$  approach  $\frac{1}{(1 - R_1)^2}$ ,  $G_2$  goes to  $G_1 - 2R_1$  and the  $\cos \theta$  expression reduces to

$$\cos \theta = \frac{R_1 - \sqrt{(R_1 - G_1)^2}}{G_1} = 1$$

which is consistent with  $R_1 > G_1$  or  $G_1$  negative, and gives a value of  $\theta = 0^\circ$  as it should.

The extreme values of the nutation angle in a given cycle of  $\alpha$  is of interest and they can be obtained by differentiating Equation 34 with respect to  $\alpha$ , solving for  $\frac{d\theta}{d\alpha}$ :

$$\frac{d\theta}{d\alpha} = \frac{(C/A - C/B) \sin \alpha \cos \alpha \sin \theta}{R_1 - G_1 \cos \theta} \quad (38)$$

and noting what values of  $\alpha$  make  $\frac{d\theta}{d\alpha}$  equal to zero. From Equation 38 it is readily seen that this occurs when

$$\alpha = 0, \pi, \pm\pi/2; \text{ for } \theta \text{ any value.}$$

It will also be noted that  $\frac{d\theta}{d\alpha}$  is zero for

$$\theta = 0, \pi; \alpha \text{ any value}$$

which, of course, are the equilibrium points. To ascertain if the extreme values are a maximum, or a minimum, the second derivative must be evaluated at the point. The second derivative,  $\frac{d^2\theta}{d\alpha^2}$ , evaluated for sign is

$$\text{sign } \frac{d^2\theta}{d\alpha^2} = \text{sign } \frac{(C/A - C/B)}{R_1 - G_1 \cos \theta} \cos 2\alpha \sin \theta \Big|_{\substack{\alpha=0 \\ \alpha=\pi/2}} \quad (39)$$

As is known, if the sign of the second derivative is negative, then the extreme value is a maximum; if the sign is positive, then it is a minimum. Thus, for  $A < B < C$  and  $\theta$  less than  $90^\circ$ , the extreme values, if they exist, are given by

$$\cos \theta_{\max} = \frac{R_1 - \text{SQRT} [R_1^2 + (1 - C/B)(1/R_2 - R_1^2 - C/B)]}{1 - C/B} \quad (40)$$

and

$$\cos \theta_{\min} = \frac{R_1 - \text{SQRT} [R_1^2 + (1 - C/A)(1/R_2 - R_1^2 - C/A)]}{1 - C/A} \quad (41)$$

For  $R_1 = 0$ , no rotor rotation, Equations 40 and 41 reduce to the classical values of

$$\sin \theta_{\max} = \sqrt{\frac{BC}{B-C} \left( \frac{1}{C} - \frac{1}{H^2/2T} \right)} \quad (42)$$

and

$$\sin \theta_{\min} = \sqrt{\frac{AC}{A-C} \left( \frac{1}{C} - \frac{1}{H^2/2T} \right)} \quad (43)$$

as it should (Reference 6). It is of interest to note that for  $\cos \theta$  to be real in Equations 40 and 41, the quantity in the square root sign must be greater or equal to zero. This requirement can be manipulated into the following inequalities:

$$R_2 \geq \frac{B}{C} \frac{(C/B - 1)}{(R_1^2 + C/B - 1)}$$

and

$$R_2 \geq \frac{A}{C} \frac{(C/A - 1)}{(R_1^2 + C/A - 1)}$$

which is consistent with previously derived bounds on  $R_2$ . For  $A < B < C$  and for motion about the  $\theta = 0^\circ$  point, it follows that  $R_2$  is bounded by the following relationship

$$\frac{B}{C} \frac{(C/B - 1)}{(C/B - 1 + R_1^2)} \leq R_2 \leq \frac{1}{(1 - R_1)^2} \quad (44)$$

Notice that if  $R_1 = 0$ , then Equation 44 reduces to the classical result

$$\frac{B}{C} \leq R_2 \leq 1$$

or

$$B \leq \frac{H^2}{2T} \leq C \quad (45)$$

#### 4. ENERGY DISSIPATION ON THE MAIN SPACECRAFT

The energy dissipation on the main spacecraft caused by a fluid ring damper will now be included in the analysis in a simple manner. Reference 7 developed the optimized energy dissipation of the damper per cycle of excitation and it is given by the following expression



$$\Delta T = -1.2 m a^2 \omega^2 \quad (46)$$

where

$m$  = mass of the fluid

$a$  = radius of the ring damper

$\omega$  = amplitude of excitation

Implied above is that the change (decrease) of spacecraft rotational energy (Equation 5) is caused by the damper. Reference 8 shows this to be valid. If the damper is put on the 2 axis, then

$$\omega = \omega_2 = \frac{H}{B} \sin \theta \sin \alpha \quad (47)$$

Now a cycle of excitation occurs when  $\alpha$  goes from 0 to  $2\pi$ . Dividing Equation 46 by  $2\pi$  and calling this  $\frac{dT}{d\alpha}$ , we have

$$\frac{dT}{d\alpha} = \frac{-1.2}{2\pi} m a^2 \omega_2^2 \quad (48)$$

Substituting Equation 47 into Equation 48 and symbolically carrying out the integration results in

$$T = T_0 - 0.19 m a^2 \frac{H^2}{B^2} \int_0^\alpha \sin^2 \theta \sin^2 \alpha d\alpha \quad (49)$$

Where  $T_0$  is the initial rotational energy of the spacecraft. Forming the dimensionless quantity  $R_2 = H^2/2TC$  gives

$$R_2 = \frac{R_{20}}{\left[ 1 - 0.38 R_{20} R_3 \int_0^\alpha \sin^2 \theta \sin^2 \alpha d\alpha \right]} \quad (50)$$

Where  $R_{20}$  is the initial value of  $R_2$  and

$$R_3 = \frac{m a^2 C}{B^2} \quad (51)$$

a dimensionless quantity containing damper and spacecraft parameters.

Now in most dynamic analyses, the initial nutation angle is given and not  $R_{20}$ . Using Equation 34,  $R_{20}$  can be calculated if the initial nutation angle,  $\theta_0$ , initial azimuth angle,  $\alpha_0$ , and other spacecraft parameters are specified. Thus,

$$R_{20} = \frac{1}{(G_{10} \cos^2 \theta_0 - 2R_1 \cos \theta_0 + R_1^2 - G_{10} + 1)} \quad (52)$$

where

$$G_{10} = 1 - \frac{C}{A} \cos^2 \alpha_0 - \frac{C}{B} \sin^2 \alpha_0$$

In using Equation 52, the maximum value of  $R_{20}$  should be used (which occurs at  $\alpha_0 = 0$  or  $\pi/2$ ) to circumvent square root of negative numbers when calculating the nutation angle. Square root of negative numbers indicates that the trajectory is not realizable.

An interesting aside can be obtained by deriving a small nutation angle damping time constant for the damper and spacecraft. Using

$$\cos \theta \approx 1 - \frac{1}{2} \sin^2 \theta,$$

Equation 34 can be written as

$$\sin^2 \theta \approx \frac{(1 - R_1)^2 - 1/R_2}{G_1 - R_1} \quad (53)$$

Substituting Equation 50 for  $R_2$  into Equation 53, differentiating with respect to  $\alpha$  to clear the integral, canceling where appropriate and averaging over a cycle considering  $\theta$  quantities constant, one obtains

$$\frac{d\theta}{d\alpha} = \frac{-0.19 R_3 \theta}{(2R_1 + C/A + C/B - 2)} \quad (54)$$

Now for  $\theta$  small, one can physically identify  $\alpha$  with time by the following expression

$$\alpha \approx \lambda t \quad (55)$$

where  $t$  = time and  $\lambda$  is the body fixed nutation frequency given by

$$\lambda = \text{SQRT} \left[ \frac{(h - (B - C) \omega_3)}{A} \frac{(h + (C - A) \omega_3)}{B} \right] \quad (56)$$

where  $\omega_3$  is considered constant. Equation 56 was obtained from Equations 2 and 3 by considering  $\omega_1$  and  $\omega_2$  varying sinusoidally with  $\lambda t$ . Thus by proper substitutions in Equation 54, a damping time constant can be determined

$$\tau = \frac{B^2(2R_1 + C/A + C/B - 2)}{0.19 \text{ m a}^2 C \lambda} \quad (57)$$

Note that the numerator of the time constant contains the sum of the left hand side of the inequalities (Equation 30a, b) needed for stable motion about the  $\theta = 0^\circ$  point. If the numerator is close to zero (implying a short time constant) then the expression is not valid because the basic assumption of slowly varying quantities is not true.

## 5. NUMERICAL RESULTS

For the special case where the angular momentum vector moves about the principal axis that contains the momentum wheel, a simple computer program was generated to calculate nutation angle trajectories and other key quantities using the IBM Continuous System Modeling Program (CSMP, Appendix A). The program inputs are: spacecraft moments of inertia, A, B, C, relative angular momentum ratio of the rotor,  $R_1$ , damping parameter,  $R_3$ , and an initial azimuth angle,  $\alpha_0$ , and an initial nutation angle,  $\theta_0$ , to specify the initial orientation of the momentum vector. The program calculates  $R_2$  and picks the trajectory ( $K = \pm 1$ ) that will give an initial nutation angle similar to the input value. The author choose this procedure over the classical method specifying  $R_2$  and letting the nutation angle occur where it may. The initial nutation angle has more physical meaning to the analyst than  $R_2$ . As previously noted, care must be used in choosing  $\alpha_0$  to circumvent square root of negative numbers.

The following spacecraft properties were used in the numerical calculations:

A = 91 mass units	C/A = 1.1538
B = 100 mass units	C/B = 1.05
C = 105 mass units	$R_3 = 0.0, 0.1$

Figure 3 shows a polar plot of nutation angle versus the free variable  $\alpha$  for small motion about the  $\theta = 0^\circ$  point,  $R_1 = 0.03$ , without and with damping. Motion is stable, periodic without damping as expected, and tends toward zero with energy dissipation.

Figure 4 shows a Cartesian plot of nutation angle versus the free variable  $\alpha$  for  $R_1 = 0.03$  and  $R_3 = 0.1$  for various initial nutation angles. It will be noticed that some curves go to the  $\theta = 0^\circ$  equilibrium point while others go to the  $\theta = 180^\circ$  point. The local peaks and valleys of the curves are mainly due to the asymmetric moments of inertia. Computer runs showed that if  $\theta_0$  were greater than  $127^\circ$ , motion would be toward the  $180^\circ$  point. If  $\theta_0$  were less than  $127^\circ$ , motion was toward the  $\theta = 0^\circ$  point. It is interesting to note that  $\theta = 126.87^\circ$  is the calculated equilibrium point (Equation 19) near the 2 axis. The equilibrium point ( $\theta = 0^\circ$  or  $180^\circ$ ) is obviously not unique and the spacecraft can capture right side up or upside down (so to speak) depending on the initial conditions.

Figure 5 shows what happens when  $R_1$  is increased to 0.09. Only the curves for  $\theta_0 = 135^\circ$  and  $170^\circ$  are shown, since the omitted curves went to the  $\theta = 0^\circ$  point previously. It will be observed that both curves now go toward the  $\theta = 0^\circ$  point. By increasing  $R_1$  to 0.09, the inequality of Equation 32b is satisfied and thus, motion about the  $\theta = 180^\circ$  point moves hyperbolically away, toward the  $\theta = 0^\circ$  equilibrium point with energy dissipation. Computer simulations with energy dissipation have shown that when the negative sign trajectory (Equation 37,  $K = -1$  in the program) is present, invariably the motion is toward the  $\theta = 0^\circ$  equilibrium point. When the positive sign trajectory is present ( $K = 1$ ) invariably the motion is toward the  $\theta = 180^\circ$  equilibrium point.

## 6. SUMMARY

It is felt that the attitude dynamics for torque-free, asymmetric dual-spin spacecraft has been developed in a straight forward and elementary manner. Analytic expressions have been developed that give results that agree with previously published dual-spin results and that reduce

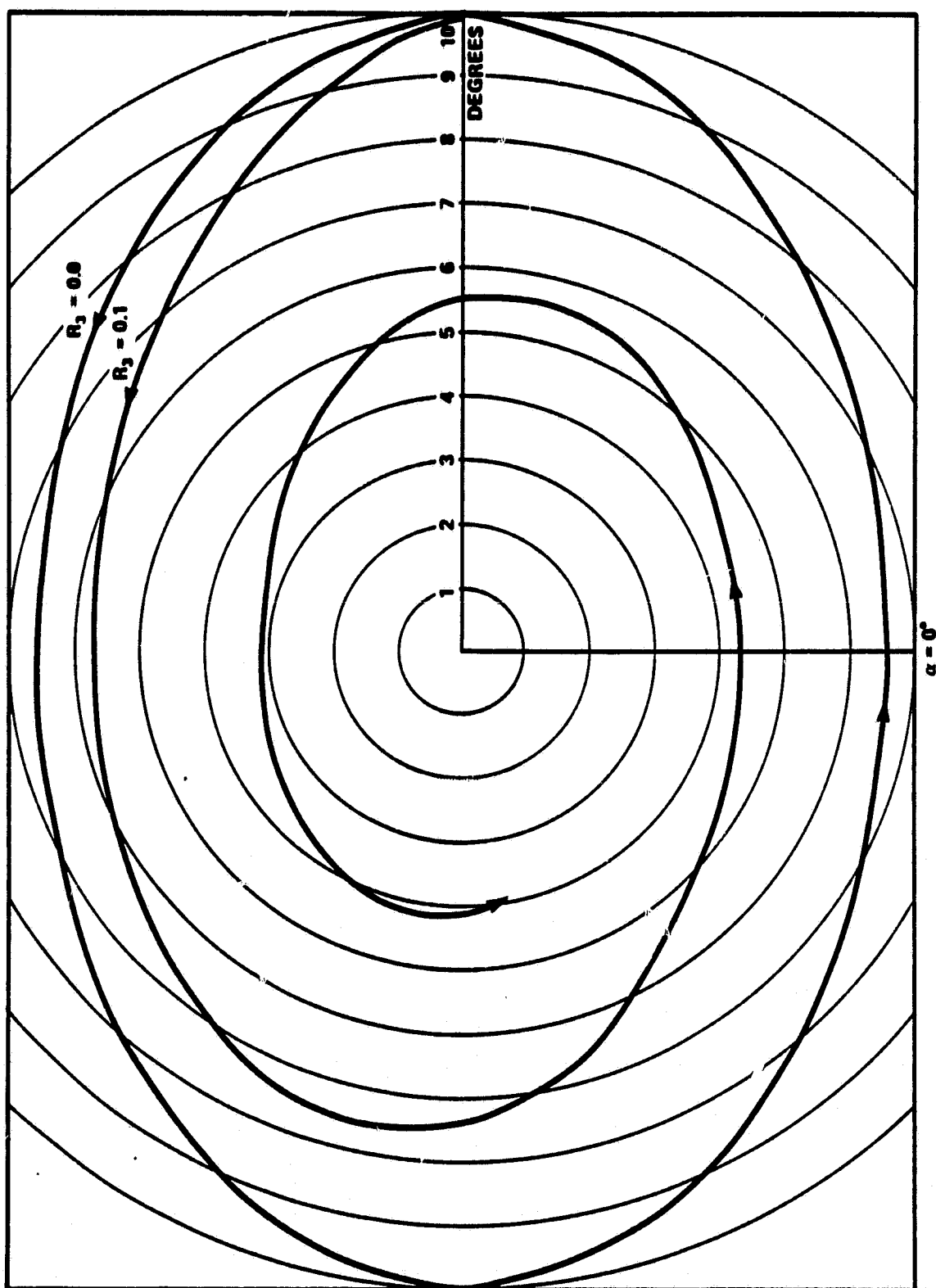


Figure 3. Polar plot of nutation angle versus free variable,  $\alpha$ , for small motion about the  $\theta = 0^\circ$  point,  $R_1 = 0.03$ ,  $R_3 = 0.0, 0.1$ .

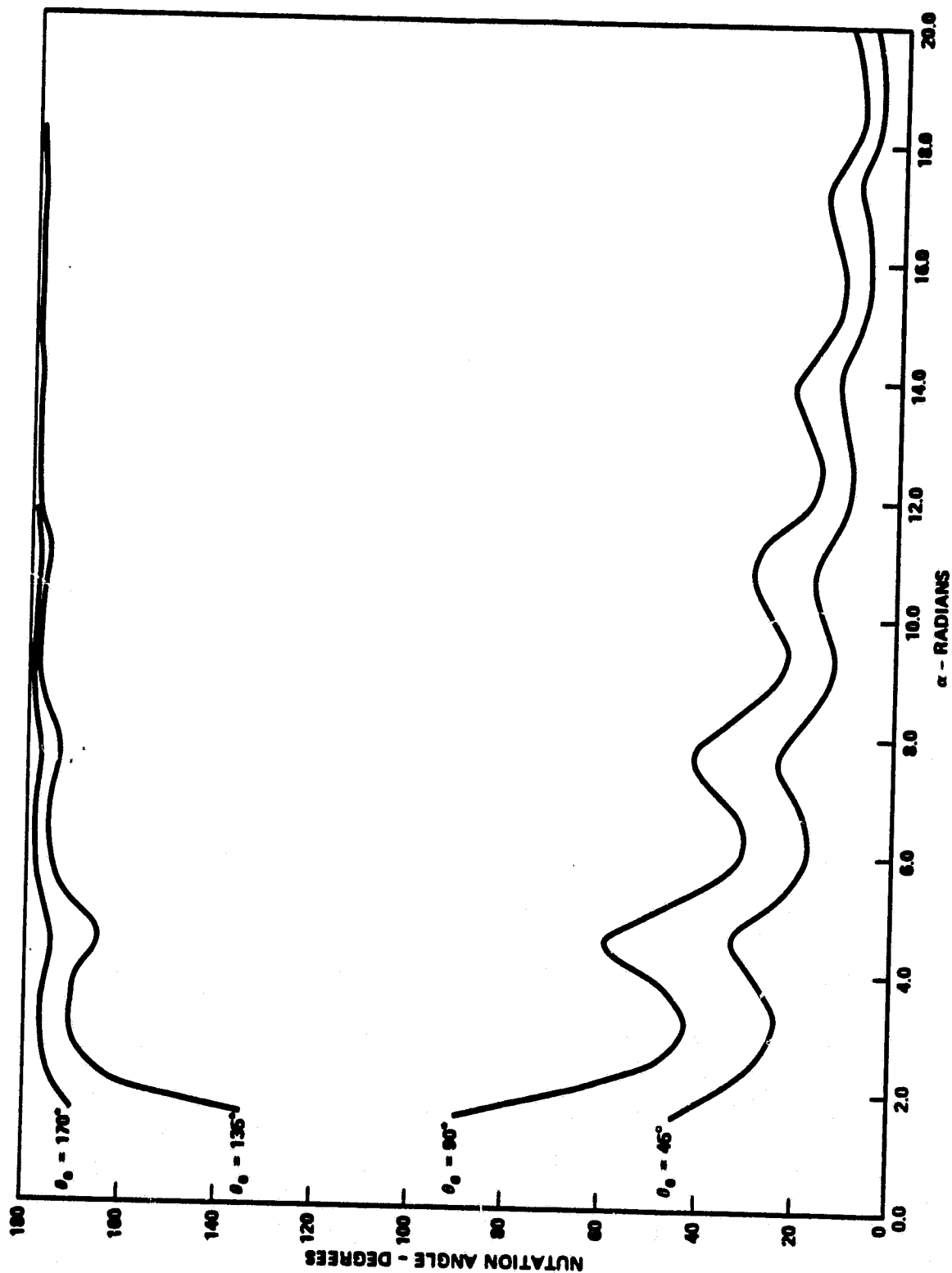


Figure 4. Nutation angle versus free variable,  $\alpha$ , for  $R_1 = 0.03$  and  $R_3 = 0.1$ , for  $\theta_0 = 45^\circ, 90^\circ, 135^\circ, 170^\circ$ .

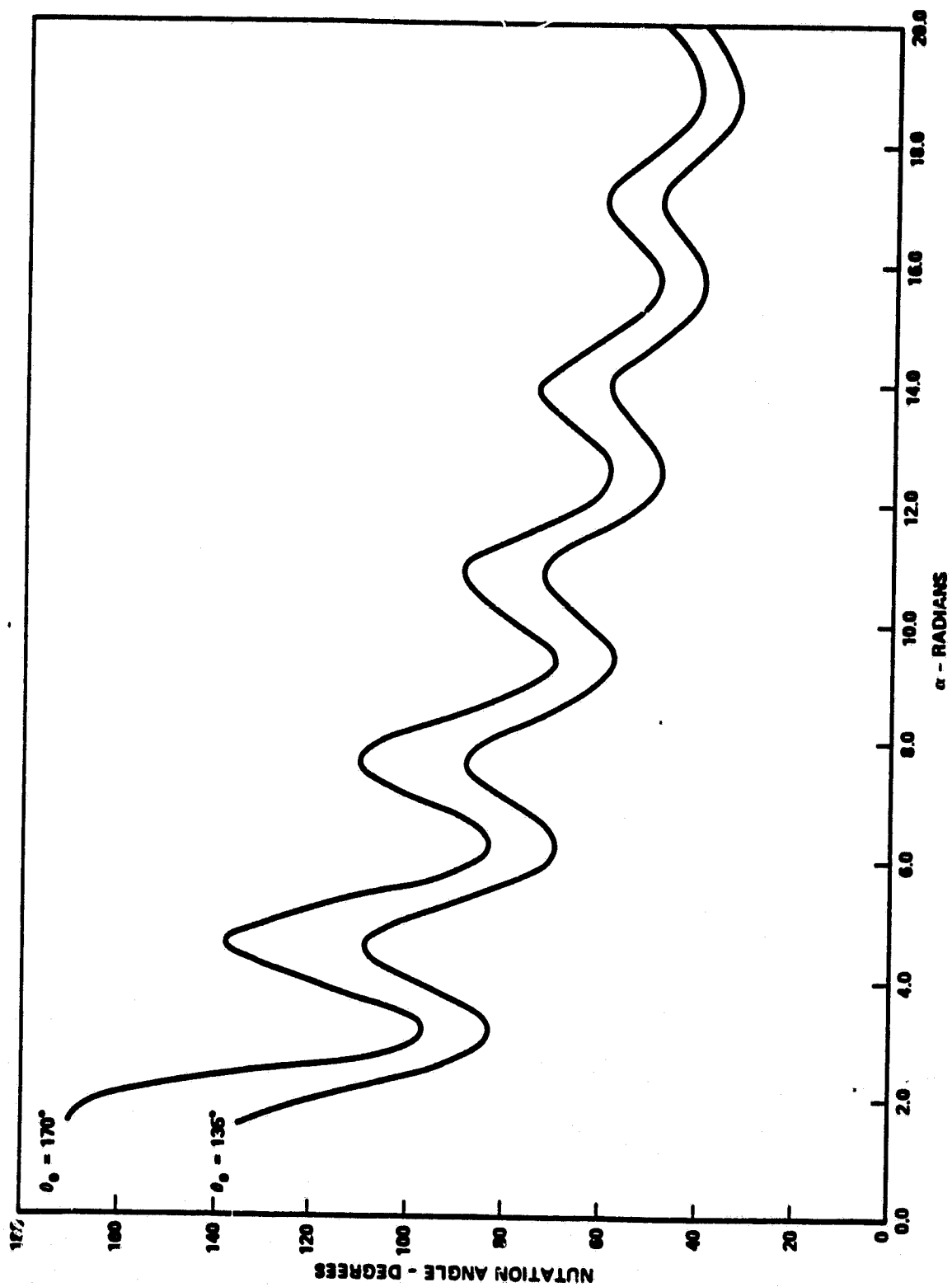


Figure 5. Nutation angle versus free variable,  $\alpha$ , for  $R_1 = 0.09$  and  $R_3 = 0.1$ , for  $\theta_0 = 135^\circ, 170^\circ$ .

to classical results for torque-free spinning spacecraft. Thus, the neophyte analyst can study dual-spin and spinning spacecraft attitude dynamics in a more or less uniform manner. The associated computer program allows the neophyte analyst to study dual-spin and simple spinning attitude motion with and without damping.

## **7. REFERENCES**

- 1. Hubert, C., "Spacecraft Attitude Acquisition from an Arbitrary Spinning or Tumbling State," Journal of Guidance & Control, Vol. 4, No. 2, March-April 1981, pp. 164-170.**
- 2. Likins, P. W., "Attitude Stability Criteria for a Dual-Spin Spacecraft," Journal of Spacecraft and Rockets, Vol. 4, April 1967, pp. 1638-1643.**
- 3. Mingori, D. L., "Effect of Energy Dissipation on the Attitude Stability of Dual-Spin Satellites," AIAA Journal 7(1), p. 20, 1969.**
- 4. Velman, J. R., "Attitude Dynamics of Dual-Spin Satellites," Hughes Aircraft Company SSD 60419R, Culver City, Calif., 1966.**
- 5. Flatley, T. W., "Equilibrium States for a Class of Dual-Spin Spacecraft," NASA Technical Report, TRR-362, March 1971.**
- 6. Kaplan, M. H., Modern Spacecraft Dynamics and Control, John Wiley & Sons, New York, 1976.**
- 7. Bhuta, P. G., and Koval, L. R., "A Viscous Ring Damper for a Freely Precessing Satellite," Int. J. Mech. Sci., Pergamon Press Ltd., 1966, Vol. 8, pp. 383-395.**
- 8. Hubert, C., "The Use of Energy Methods in the Study of Dual-Spin Spacecraft," Proceedings of AIAA Guidance and Control Conference, Danvers, Mass., August 1980, pp. 372-375.**



# APPENDIX A

## CSMP PROGRAM FOR MOTION OF THE ANGULAR MOMENTUM VECTOR ABOUT THE AXIS THAT CONTAINS THE MOMENTUM WHEEL

\*\*\*\*CONTINUOUS SYSTEM MODELING PROGRAM\*\*\*\*

\*\*\* VERSION 1.3 \*\*\*

```

TITLE DUAL SPIN SPACECRAFT WITH JAMMING
INITIAL
PARAMS A=91.0,B=100.0,C=105.0,R1=0.01
PARAMS R3=0.1
PARAMS THETD0=(10.0,45.0,90.0,135.0,170.0)
CONSTANT A0=1.5708
THETO = THETD0/57.297
NUM1 = (A/C)*(C/A - 1.)
DENOT = R1/R1 + C/A - 1.
R2LO1 = NUM1/DENOT
NUM2 = (B/C)*(C/B - 1.)
DENOT2 = R1/R1 + C/B - 1.
R2LO2 = NUM2/DENOT2
H00007
CTHET = COS(THETO)
G10 = 1.-(C/A)*(COS(A0))**2-(C/B)*(SIN(A0))**2
DEN3 = G10*(CTHET)**2 - 2.*R1*CTHET*R1*R1-G10+1.
R20 = 1./DEN3
G20 = (1./R20) - R1/R1 + G10 - 1.
F10 = R1*SQRT(R1*R1+G10*G20)
CO1 = F10/G10
Y1 = ABS(CO1-CTHET)
F20 = R1-SQRT(R1*R1+G10*G20)
CO2 = F20/G10
Y2 = ABS(CO2-CTHET)
IF(Y1,LT,Y2) GO TO 1
1 K=1.0
2 GO TO 3
3 CONTINUE..
DYNAMIC
ALPH = ALP+A0
R2 = R20/DIS
DIS = 1.-0.38*R3*R20*INT
INT = INTGR(0.0,ANG)
ANG = (SIN(THET))*(SIN(THET))*(SIN(ALPH))*(SIN(ALPH))
NORM1 = (SIN(THET))*COS(ALPH)
NORM2 = (SIN(THET))*SIN(ALPH)
NORM3 = COS(THET)
THET = ARCCOS(ARG)
ARG = F1/G1
F1 = R1+K*SQRT(R1*R1+G1*G2)
G1 = 1.-(C/A)*(COS(ALPH))**2-(C/B)*(SIN(ALPH))**2
G2 = (1./R20) - R1/R1 + G1 - 1.
FIR = R1/R1+G1*G2
THETD = 57.297*THET
G12 = G1*G2
ARF = ANG/57.297
A00 = A0+57.297
FINISH ARF= 9.9999E-01,FIR=0.3E-07
RENAME TIME = ALP
TERMINAL
METHOD RKSPX
A0 = 0.0
5 G10 = 1.-(C/A)*(COS(A0))**2-(C/B)*(SIN(A0))**2
G20 = (1./R20) - R1/R1 + G10 - 1.
F10 = R1/R1 + G10*G20
A00 = A0+57.297
WRITE(6,10) A0,F10
10 FORMAT(1H0,'A00=' ,E12.5,3X,'F10=' ,E12.5)
IF((A0-3.1416).GT.0.) GO TO 7
A0 = A0+0.05
GO TO 5
7 CONTINUE
A0 = 1.5708
TIMER FINTIM= 20.0,DELT=0.15,OUTDEL=0.15
PRINT ALPH,THETD,R2,FIR,G12,DIS,ARG,G2,K,G1,A00,Y1,Y2,R2LO1,R2LO2
PLOT THETD
END
STOP

```